


Low-Energy Nuclear Excitations along the α -Decay Chains of Superheavy ^{292}Lv and ^{294}Og

J. Luis Egido^{1,*} and Andrea Jungclaus^{2,†}

¹*Departamento de Física Teórica and CIAFF, Universidad Autónoma de Madrid, E-28049 Madrid, Spain*

²*Instituto de Estructura de la Materia, CSIC, E-28006 Madrid, Spain*

 (Received 8 February 2021; revised 5 April 2021; accepted 15 April 2021; published 10 May 2021)

We present the first triaxial beyond-mean-field study of the excitation spectra of even-even superheavy nuclei. As representative examples, we have chosen the members of the α -decay chains of ^{292}Lv and ^{294}Og , the heaviest even-even nuclei which have been synthesized so far using ^{48}Ca -induced fusion-evaporation reactions. In our calculations, the effective finite-range density-dependent Gogny force is used and the angular-momentum and particle-number symmetries are restored. Configuration-mixing calculations are performed to determine ground- and excited-state deformations and to establish the collective band structures of these nuclei. Rapidly varying characteristics are predicted for the members of both decay chains, which are further accentuated when compared to the predictions of simple collective models. Based on the present calculations, the prospect of observing α -decay fine structures in future experiments is discussed.

DOI: 10.1103/PhysRevLett.126.192501

The synthesis of the superheavy elements flerovium (Fl), moscovium (Mc), livermorium (Lv), tennessine (Ts), and oganesson (Og) with proton numbers $Z = 114 - 118$ using “hot” fusion-evaporation reactions of ^{48}Ca beams on actinide targets is one of the most important achievements in physics and chemistry research in the last two decades (see Ref. [1] and references therein). The heaviest even-even nuclei ^{288}Fl , ^{292}Lv , and ^{294}Og , for example, were synthesized using the reactions $^{244}\text{Pu}(^{48}\text{Ca}, 4n)$, $^{248}\text{Cm}(^{48}\text{Ca}, 4n)$, and $^{249}\text{Cf}(^{48}\text{Ca}, 3n)$ [1]. Because of the small reaction cross sections, only very few nuclei can be produced in each experiment. It is therefore notoriously difficult to obtain experimental information beyond the α -decay half-life and energy for these superheavy nuclei (SHN). Also from the theoretical side, the study of the heaviest nuclei is a challenge. So far mainly macroscopic-microscopic models and mean-field (MF) approaches have been used to describe the properties of SHN (see Refs. [2–7] and references therein). The α -decay chains of the heaviest nuclei cross a region of the nuclear chart for which these models predict rapidly changing nuclear structure properties. In particular, several MF studies forecast a shape transition from prolate to oblate and finally spherical shapes toward the supposed neutron shell closure at $N = 184$ [4–7]. This is illustrated in Fig. 1, which shows these chains embedded in the chart of nuclides color coded according to the ground-state quadrupole deformation parameter β , positive (negative) values correspond to prolate (oblate) shapes, calculated in the Hartree-Fock-Bogoliubov (HFB) approach with the Gogny force [6]. However, it has long been speculated that triaxial shapes, as well as correlations beyond the mean field, which both are not considered in these MF calculations, may be crucial for a correct description of the transitional

superheavy nuclei [5,7,8]. Note that, from the nuclear structure point of view, the situation is much less uncertain for the lower- Z superheavy nuclei ($Z = 107-113$), which were discovered using “cold” fusion reactions [9,10]. The decay chains of these less neutron-rich nuclei pass through the region of stable quadrupole deformation centered around $^{254}\text{No}_{152}$, as exemplarily shown in Fig. 1 for the α -decay chain of ^{270}Ds [11], the heaviest even-even isotope synthesized using cold fusion reactions.

Recently, a milestone in experimental SHN research was reported. The detection of an α -electron coincidence following the decay of ^{286}Fl meant the first observation of the decay of an excited state in an even-even superheavy

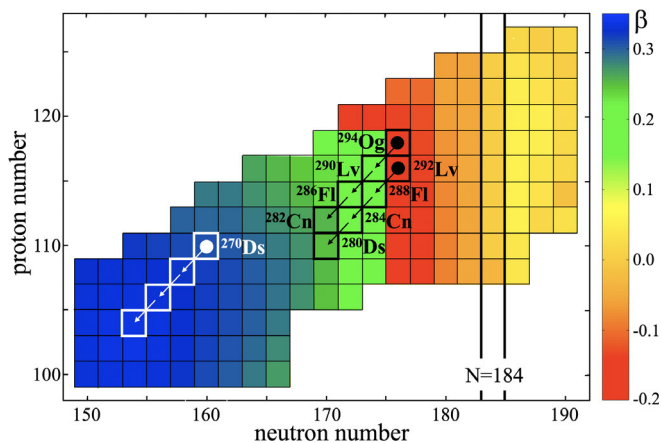


FIG. 1. HFB ground-state quadrupole deformation parameters β for even-even SHN (adapted from Ref. [6]). The α -decay chains of interest are shown as black squares.

nucleus, namely ^{282}Cn [12]. Motivated by this achievement, an exploratory study of SHN using the state-of-the-art triaxial-symmetry-conserving configuration-mixing (SCCM) approach (see Refs. [13,14] and references therein) with effective nuclear forces was presented [15]. This SCCM study of the even $^{288-298}\text{Fl}$ isotopes has dramatically revised the picture delineated by the axial-symmetric MF calculations. Instead of a prolate-oblate-spherical shape transition (see Fig. 1), the SCCM calculations predict six different ground-state deformations (prolate, triaxial with $\gamma \sim 20^\circ$, $\gamma \sim 40^\circ$, and $\gamma \sim 30^\circ$, respectively, oblate and spherical) for the six studied isotopes.

The recent progress suggests that a detailed understanding of this fascinating region of the nuclear landscape may come within reach once substantially increased production rates become available at the new generation of dedicated facilities for SHN research. Here, we present the first realistic predictions of the excitation schemes of the experimentally accessible α -decay chains of ^{292}Lv and ^{294}Og to provide theoretical guidance for future experimental studies.

The SCCM approach considers linear combinations of symmetry-conserving product wave functions generated by considering the deformation parameters as coordinates, i.e.,

$$|\Phi_M^{I\sigma}\rangle = \sum_{\{\xi,K\}} f_{\{\xi,K\}}^{I\sigma} P^Z P^N P_{MK}^I |\phi(\xi)\rangle, \quad (1)$$

where $\{\xi\}$ represents the shape parameters $\{\beta, \gamma\}$. The operators P^Z , P^N , and P_{MK}^I are projector operators associated with the particle number (Z for protons and N for neutrons) and the angular momentum, respectively, see Ref. [13]. $\sigma = 1, 2, \dots$ labels the states for a given value of the angular momentum I . The quantum numbers M and K are the projections of \vec{I} on the laboratory and intrinsic z axes, respectively. The Hartree-Fock-Bogoliubov wave functions $|\phi(\xi)\rangle$ of Eq. (1) depend parametrically on the deformation. To determine them, and in order to avoid the pairing collapse, we perform the particle-number restoration in the variation-after-projection approach (PNVAP) [14] instead of the usual HFB minimization. Finally, the coefficients $f_{\{\xi,K\}}^{I\sigma}$ of the linear combination in Eq. (1) are determined by a minimization of the energy. In all calculations, the finite-range density-dependent Gogny force [16] in its D1S parametrization [17] is used together with a configuration space of thirteen major harmonic oscillator shells. Further technical details of the calculations are provided in Ref. [15].

We start the discussion with the presentation of the particle-number projected (PNVAP) potential-energy surfaces (PES) in the (β, γ) plane for ^{292}Lv , ^{288}Fl , ^{284}Cn , and ^{280}Ds , the members of the α -decay chain of ^{292}Lv , shown in the left column of Fig. 2. The α -decay branch to ^{280}Ds was established only very recently [12]. We note that the PES of the respective isotones with $Z + 2$, i.e., the members of the

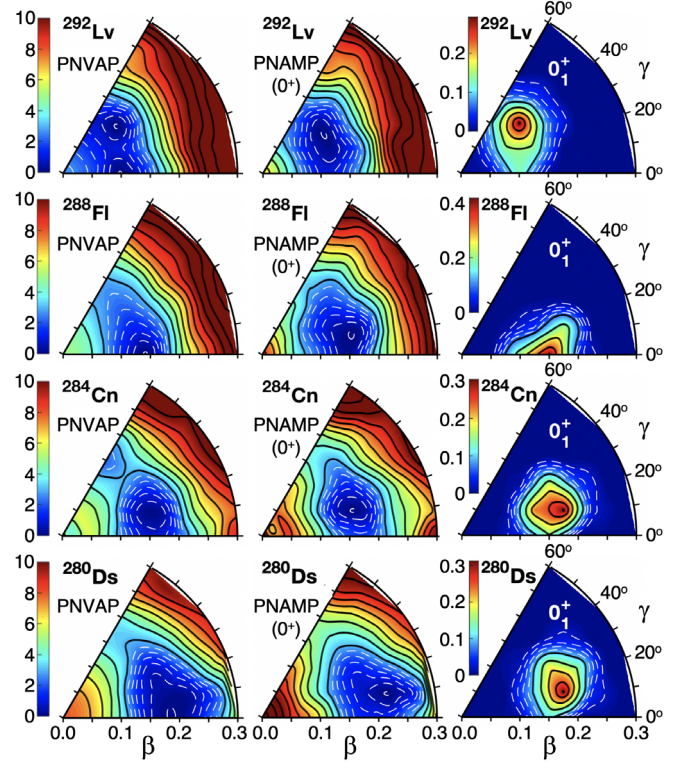


FIG. 2. PNVAP (left), $I = 0\hbar$ PNAMP (middle) PES and squared collective wave functions of the 0^+ ground states (right) for ^{292}Lv , ^{288}Fl , ^{284}Cn , and ^{280}Ds . The palettes to the left are common for the panels of the first two columns. The PES are normalized to the minimum of each surface and the dashed white and solid black contour lines are separated by 0.5 and 1.0 MeV, respectively. In the last column, the dashed white contour lines display probability densities of 0.02, 0.04, 0.06, and 0.08 while the solid black lines uniformly cover the range between 0.1 and the maximum value displayed in the corresponding palette.

^{294}Og decay chain, look very similar since the dependence of the shape evolution on the atomic number Z is weak (compare Fig. 1). Considering only axial-symmetric shapes, coexisting prolate ($\gamma = 0^\circ$) and oblate ($\gamma = 60^\circ$) minima in the potential energy are observed for all four nuclei, with the prolate one being lower in energy. However, when triaxial shapes are taken into account some of these minima turn into saddle points and triaxial minima emerge. In the second column of Fig. 2, the PES obtained after projection to particle number and angular momentum $I = 0\hbar$, PNAMP, are shown. In all cases, triaxial minima are found in the projected surfaces with triaxiality parameters in the range $\gamma = 10^\circ - 35^\circ$ and quadrupole deformations which are smoothly increasing from $\beta \sim 0.11$ in ^{292}Lv to $\beta \sim 0.22$ in ^{280}Ds . The existence of these minima, however, does not necessarily imply that all these nuclei are triaxial in their ground states. To unequivocally determine the ground-state deformation of these soft nuclei, configuration-mixing calculations have to be performed. The third column of Fig. 2 shows the collective wave functions, i.e., the probability densities in the (β, γ) plane, of

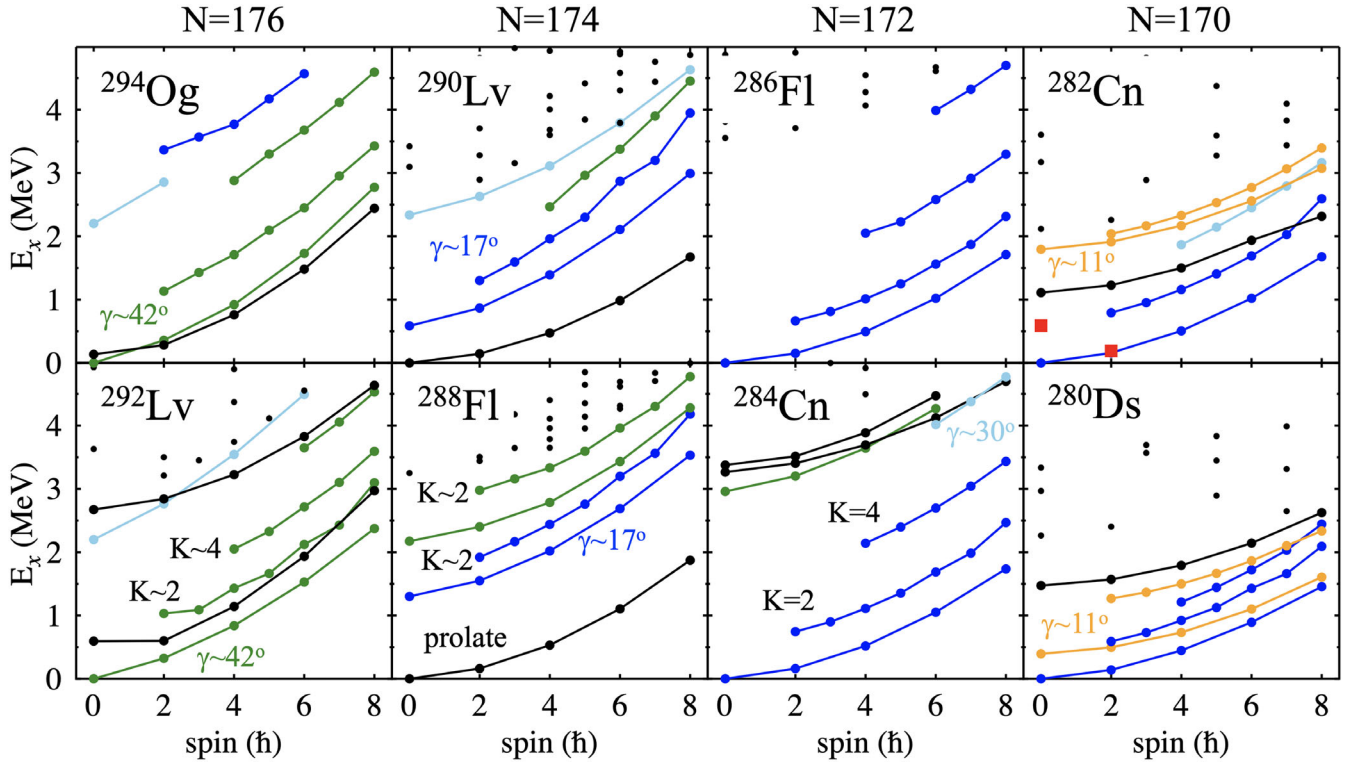


FIG. 3. Excitation energy versus angular-momentum plots for the band structures of the members of the α -decay chains of ^{294}Og (top row) and ^{292}Lv (bottom row). Prolate bands are shown in black while triaxial bands are plotted in orange ($\gamma \sim 11^\circ$), blue ($\gamma \sim 17^\circ$), sky blue ($\gamma \sim 30^\circ$), and green ($\gamma \sim 42^\circ$). Some $K > 0$ bands are labeled by the dominant K value. Dots mark the positions of additional calculated states and the red squares indicate the experimental excitation energies of the 2_1^+ and 0_2^+ states in ^{282}Cn [12].

the ground states of the four nuclei under study. For ^{292}Lv , ^{284}Cn , and ^{280}Ds , the wave functions peak around the (β, γ) values at which the potential-energy minimum is found. Only in the case of ^{288}Fl , the barrier toward axial symmetry in the PNAMP PES turned out to be too low to maintain a triaxial shape of the ground state. Configuration mixing drives the nucleus toward a prolate ground-state deformation. To summarize, only one of the four nuclei under study, namely the prolate ^{288}Fl , indeed exhibits in the triaxial calculations the shape expected on the basis of the axial-symmetric MF calculations (see Fig. 1). The other three are predicted to be triaxial in their ground states.

In the following, we will investigate the excitation schemes, i.e., the collective band structures, of the nuclei under study. Configuration-mixing calculations were performed for angular momenta up to $I = 8\hbar$. The resulting excited states were grouped into bands according to similarities of the wave functions. The assigned bands are displayed in the excitation energy versus angular-momentum plots of Fig. 3. Already at first sight it is obvious that the different ground-state deformations of the members of each decay chain result in very different band structures. We will limit the discussion to the members of the ^{292}Lv chain since the excitation spectra of the respective isotones in the ^{294}Og chain are rather similar. In ^{292}Lv , above

the triaxial ground-state band (GSB), a prolate band is predicted at low excitation energy in addition to $K \approx 2$ and $K \approx 4$ bands which have the same shape as the GSB. The interaction between these close-lying bands leads to strong K mixing and staggering effects. For the $N = 174$ nucleus ^{288}Fl collective bands based on triaxial 0_2^+ ($\gamma \sim 17^\circ$) and 0_3^+ ($\gamma \sim 42^\circ$) states are predicted roughly 1.3 and 2.2 MeV above the prolate GSB. Both are accompanied by $K \approx 2$ bands of similar shape. A clearly different pattern is obtained for the $N = 172$ nucleus ^{284}Cn . In this case, the second and third 0^+ states of triaxial ($\gamma \sim 42^\circ$) and prolate shape, respectively, are much higher in energy, close to 3 MeV, so that at low energy the excitation scheme is dominated by the triaxial GSB ($\gamma \sim 17^\circ$) and the corresponding $K \approx 2$ and $K \approx 4$ bands. Finally, the first excited band in ^{280}Ds , of triaxial shape with $\gamma \sim 11^\circ$, is predicted as low as 0.4 MeV above the triaxial GSB ($\gamma \sim 17^\circ$). In addition to the $K \approx 2$ and $K \approx 4$ bands belonging to the triaxial bands, a prolate band is expected 1.5 MeV above the yrast line.

The results of our calculations presented in the Figs. 2 and 3 clearly demonstrate that the consideration of triaxial shapes as well as correlations beyond the mean field is mandatory for a realistic description of the properties of SHN. While the axial-symmetric MF calculations mentioned

in the introduction systematically predict the coexistence of prolate and oblate shapes for many $N = 172 - 182$ isotones, Fig. 3 illustrates that in the more realistic calculations presented here in general triaxial shapes dominate and in most cases even more than two configurations of different shape compete. This rich variety of shapes and configurations is a direct consequence of the high density of single-particle states in these heavy nuclei and the occurrence of relatively small energy gaps which are varying as a function of β and γ (see Fig. 5 of Ref. [5]).

The calculations we presented in this Letter are of a purely microscopic nature, starting from a global nucleon-nucleon interaction and using the generator coordinate method with full triaxial angular-momentum and particle-number projection. Although this approach is diametrically opposed to the somewhat simplistic nature of the collective models, which are often used to classify atomic nuclei, it is interesting to confront our results to the predictions of the latter. The PNVAP PES shown in Fig. 2 indicate an axial-symmetric prolate minimum for ^{288}Fl , a γ -soft potential for ^{292}Lv , and finally triaxial deformation for ^{284}Cn . Nuclei with potentials of these characteristics are commonly described in the framework of three different models: the axial-symmetric rotor model of Bohr and Mottelson [18], the γ -unstable triaxial rotor model proposed by Willets and Jean [19], and the rigid triaxial rotor model introduced by Davydov [20,21]. The predictions of these models for the excitation energies of the members of the collective bands, normalized to the energy of the 2_1^+ state, are shown in Fig. 4. For an axial-symmetric rotor, a regular rotational band with $E_x \sim I(I+1)$ is expected with an energy ratio $R = E(4_1^+)/E(2_1^+) = 3.3$. The spectrum of a

γ -unstable nucleus is predicted to be more compressed ($R = 2.5$). Besides the GSB, the Willets-Jean model predicts a low-lying $K = 2$ band with strong odd-even staggering. Finally, for a rigid triaxial rotor, the excitation energies depend on the value of the triaxiality parameter γ as illustrated in Fig. 4. While for small values of γ the excitation energies within the GSB are very close to those of an axial-symmetric rotor, they significantly decrease for larger values of γ approaching the predictions for a γ -unstable nucleus. The most striking feature of the Davydov model, though, is the prediction of $K = 2$ and $K = 4$ bands with rapidly decreasing excitation energies with increasing values of γ . In the past, energy ratios such as R and $E_x(2_2^+)/E_x(2_1^+)$, as well as quantities related to the staggering of the $K = 2$ band, were extensively used to classify the excitation spectra of even-even nuclei [22–24]. Fig. 4 shows that the calculated GSB of ^{288}Fl ($R = 3.28$) nicely follows the pattern expected for an axial-symmetric rotor. In the case of ^{292}Lv with $R = 2.59$, the level sequence of the GSB is much closer to the limit of the γ -unstable rotor, consistent with the observation of a very γ -soft potential-energy surface (see Fig. 3). We note, however, that this PES exhibits two minima while the model assumes a potential which is completely flat in the γ degree of freedom. The interaction between the low-lying triaxial and prolate bands, compare Fig. 3, unfortunately prevents a meaningful comparison of the excited bands to the model predictions. Definitely the most interesting case is that of ^{284}Cn . While the value $R = 3.23$ is close to that expected for an axial-symmetric rotor, the energies of the 6_1^+ and 8_1^+ states clearly show increasing deviations from the expected pattern. They are best described by the Davydov model for a value $\gamma \sim 17^\circ$, in accord with the position of the maximum of the ground-state wave function, see Fig. 2. For the same value of γ , also the energies of the members of the $K = 2$ band are very well reproduced. The energies within the $K = 4$ band are only slightly lower than expected for $\gamma \sim 17^\circ$ and well reproduced by the model assuming $\gamma \sim 20^\circ$. This suggests that the nucleus ^{284}Cn may possibly be one of the best candidates for the manifestation of rigid triaxial rotation in nature. Note that in the even Os isotopes $^{186-192}\text{Os}$, which are since long considered as prime examples of rigid triaxial rotors, the collective $K = 4$ bands are observed at much lower excitation energies than predicted by the model [25,26]. The comparison shown in Fig. 4 highlights the diversity of shapes and structures we encountered in the region of the transitional SHN, where three nuclei, each separated only by one α particle, seem to constitute textbook examples for three different collective models. We note, however, that ^{288}Fl and ^{284}Cn are rather exceptional cases because in these nuclei the ground-state configuration is well isolated from the excited structures. In general, the microscopic calculations presented here predict a rich variety of competing configurations (see Fig. 3) which naturally is beyond the scope of simplistic models.

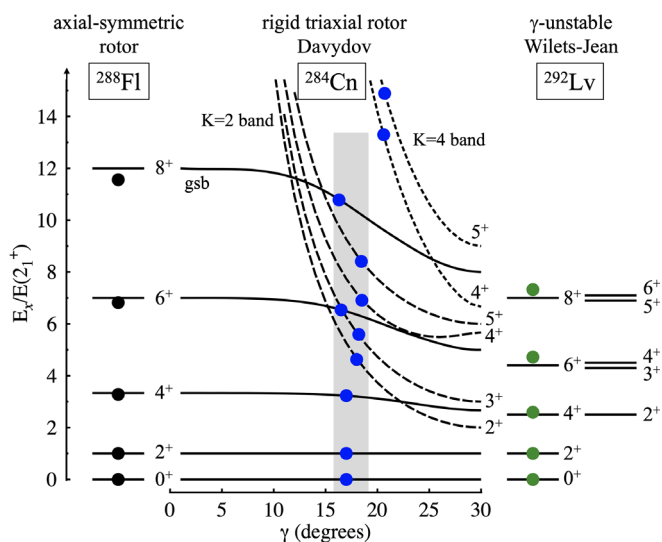


FIG. 4. Excited-state energies (black lines) predicted by the three collective models discussed in the text. The calculated energies of the excited states of ^{288}Fl (black), ^{284}Cn (blue), and ^{292}Lv (green) are included as filled circles.

As mentioned in the introduction, very recently first experimental information about excited-state energies in a transitional even-even SHN, namely ^{282}Cn , was reported [12]. As shown in Fig. 3, the energy of the 2_1^+ state nicely agrees with the theoretical expectation while the 0_2^+ state is predicted at a slightly higher excitation energy. The α decay to an excited state in ^{282}Cn was observed in one out of the 29 decays of ^{286}Fl studied so far [12]. In contrast, no such event was detected yet in the decay of ^{288}Fl , of which 51 cases were studied. Given the limited statistics available so far it is certainly premature to draw any firm conclusion. We note, however, that the nonobservation of a decay branch to excited states in ^{284}Cn in the α decay of ^{288}Fl is consistent with our prediction of a very high excitation energy of $E_x \sim 3$ MeV for the first excited 0^+ state in this nucleus. From the nuclear structure point of view, the results shown in Fig. 3 suggest that besides ^{286}Fl , its isotone ^{284}Cn and the $N = 176$ nuclei ^{294}Og and ^{292}Lv are the best candidates for the observation of α -decay fine structures.

To conclude, we presented the first triaxial beyond-mean-field study of the excitation spectra of SHN, namely the experimentally accessible members of the α -decay chains of ^{294}Og and ^{292}Lv . The results of the calculations show that a rich variety of shapes and configurations is expected to occur in the upper end of the chart of nuclides, resulting in rapidly changing structural properties. A comparison with collective models suggests ^{292}Lv , ^{288}Fl , and ^{284}Cn to be good examples for a γ -unstable triaxial rotor, an axial-symmetric prolate rotor, and a rigid triaxial rotor, respectively. The results of our calculations are in qualitative agreement with the recent observation of a fine structure in the α decay of ^{286}Fl and suggest that in ^{280}Ds , as well as the $N = 174$ isotones ^{288}Fl and ^{290}Lv , excited 0^+ states may exist at energies similar to that of the 0_2^+ level identified in ^{282}Cn . The increased beam intensities at the future SHE facilities, combined with the outstanding sensitivity of modern detection setups and theoretical guidance, open exciting perspectives for future nuclear structure research in the region of SHN.

This work was supported by the Spanish Ministerio de Ciencia, Innovación y Universidades under Contract No. FPA2017-84756-C4-2-P.

*j.luis.egido@uam.es

†andrea.jungclaus@csic.es

- [1] Yu. T. Oganessian and V. K. Utyonkov, *Rep. Prog. Phys.* **78**, 036301 (2015).
- [2] M. Bender, K. Rutz, P.-G. Reinhard, J. A. Maruhn, and W. Greiner, *Phys. Rev. C* **60**, 034304 (1999).
- [3] J.-F. Berger, L. Bitaud, J. Dechargé, M. Girod, and K. Dietrich, *Nucl. Phys.* **A685**, 1 (2001).
- [4] A. Sobczewski and K. Pomorski, *Prog. Part. Nucl. Phys.* **58**, 292 (2007).
- [5] S. Cwiok, P.-H. Heenen, and W. Nazarewicz, *Nature (London)* **433**, 705 (2005).
- [6] M. Warda and J. L. Egido, *Phys. Rev. C* **86**, 014322 (2012).
- [7] P.-H. Heenen, J. Skalski, A. Staszczak, and D. Vretenar, *Nucl. Phys.* **A944**, 415 (2015).
- [8] P.-H. Heenen, B. Bally, M. Bender, and W. Ryssens, *Eur. Phys. J. Web Conf.* **131**, 02001 (2016).
- [9] S. Hofmann and G. Münzenberg, *Rev. Mod. Phys.* **72**, 733 (2000).
- [10] K. Morita *et al.*, *J. Phys. Soc. Jpn.* **81**, 103201 (2012).
- [11] G. Münzenberg, *Nucl. Phys.* **A944**, 5 (2015).
- [12] A. Sâmark-Roth *et al.*, *Phys. Rev. Lett.* **126**, 032503 (2021).
- [13] T. R. Rodríguez and J. L. Egido, *Phys. Rev. C* **81**, 064323 (2010).
- [14] J. L. Egido, *Phys. Scr.* **91**, 073003 (2016).
- [15] J. L. Egido and A. Jungclaus, *Phys. Rev. Lett.* **125**, 192504 (2020).
- [16] J. Dechargé and D. Gogny, *Phys. Rev. C* **21**, 1568 (1980).
- [17] J. F. Berger, M. Girod, and D. Gogny, *Nucl. Phys.* **A428**, 23c (1984).
- [18] A. Bohr and B. R. Mottelson, *Nuclear Structure* (World Scientific, Singapore, 1998), Vol. II.
- [19] L. Wilets and M. Jean, *Phys. Rev.* **102**, 788 (1956).
- [20] A. S. Davydov and G. F. Filippov, *Nucl. Phys.* **8**, 237 (1958).
- [21] A. S. Davydov and V. S. Rostovsky, *Nucl. Phys.* **12**, 58 (1959).
- [22] N. V. Zamfir and R. F. Casten, *Phys. Lett. B* **260**, 265 (1991).
- [23] K. Nomura, N. Shimizu, D. Vretenar, T. Niksic, and T. Otsuka, *Phys. Rev. Lett.* **108**, 132501 (2012).
- [24] R. F. Casten, R. B. Cakirli, D. Bonatsos, and K. Blaum, *Phys. Rev. C* **102**, 054310 (2020).
- [25] J. L. Wood, A. M. Oros-Peusquens, R. Zaballa, J. M. Allmond, and W. D. Kulp, *Phys. Rev. C* **70**, 024308 (2004).
- [26] J. M. Allmond, R. Zaballa, A. M. Oros-Peusquens, W. D. Kulp, and J. L. Wood, *Phys. Rev. C* **78**, 014302 (2008).